UWB In-Body Channel Performance by Using a Direct Antenna Designing Procedure

Carlos Andreu[1], Concepcion Garcia-Pardo[1], Alejandro Fornes-Leal[1], Marta Cabedo-Fabrés[1], Narcís Cardona[1]
[1] Institute of Telecommunications and Multimedia Applications, Universitat Politècnica de València, Valencia, Spain,
caranes@iteam.upv.es

***Abstract*— UWB systems have been proposed as a candidate for the next generation of in-body applications. In order to perform reliable UWB channel measurements, implantable antennas should work in the propagation medium properly. To assess the UWB channel performance, in-body antenna matching should be assured. Besides, an omnidirectional radiation pattern in order to communicate with a sensor array located around the body should be achieved. This paper is devoted to the analysis of the UWB in-body channel when using an antenna miniaturization procedure that maintains its omnidirectional radiation pattern as well as its operation bandwidth. For that, an UWB monopole antenna with circular patch is directly miniaturized and optimized considering the human muscle tissue. To assess the impact of antenna miniaturization, the results of the channel propagation measurement campaign obtained with the miniaturized antenna are compared with those obtained from a larger UWB monopole in a previous measurement campaign.**

***Index Terms*— Body area network, Ultra-wideband (UWB), in-body communications.**

I. INTRODUCTION

Wireless body area networks (WBANs) can enable communications between independent nodes located inside the body, over the body surface or further. IEEE Std. 802.15.16, normalized the Medical Implant Communication Service (MICS) band as the frequency band (402-405 MHz) to communicate in-body devices [1]. However, this band is constrained to the use of narrow band systems up to 300 kHz. Therefore, many research works aim to consider Ultra-Wideband (UWB) technology, which covers from 3.1 to 10.6 GHz, as a good candidate in order to enhance the next generation of implantable devices [2].

Accurate UWB implant channel characterization is challenging. Implanting devices in human subjects in order to perform research works is non-viable due to health and safety reasons. In literature, some investigations have been performed in clinical facilities using porcine models [3] can be found. Nevertheless, the high-cost and the low availability of animal experimentation is a fact. Some research works attempt to characterize the UWB in-body channel by means of sophisticated electromagnetic software [4]. Nevertheless, this software needs a complex and expensive data processor. Besides, reproducing and simulating all body channel conditions can be an unrealizable task. In contrast, chemical dissolutions which imitate the dielectric features of the human body tissues (known as phantoms) could be a cost-effective solution.

In order to achieve a realistic experimental characterization of the UWB in-body channel, miniaturized antennas play a crucial role. The overall dimensions of implantable antennas should be suitable to be implanted inside the human body. Furthermore, achieving high data rates occupying the whole UWB bandwidth is one of the most relevant challenges of UWB antennas. Besides, in-body antennas should have an omnidirectional radiation pattern at all frequencies to communicate with an on-body sensor array or an external receiver. In literature, many papers where implantable antennas are designed to work in narrow band systems can be found [5] [6], although there is a lack of research works related to UWB in-body antennas. Most of implantable antenna designs take as initial designing stage the validation in free space, i.e., the antenna is miniaturized in order to work at higher frequencies than UWB [7]. Then, the antenna is wrapped with a human body tissue which has a high dielectric constant. Thus, the resonance bandwidth is shifted down since the wavelength is shorter [8]. However, this miniaturization approach is not efficient in antennas with large bandwidth due to the frequency dependence of dielectric features of body tissues. As a consequence, the antenna characteristics such as radiation pattern and impedance bandwidth may not be as expected.

This work is devoted to the characterization of UWB in-body channel. For this purpose, a coplanar waveguide fed UWB monopole has been miniaturized and optimized by taking into account directly the dielectric properties of body tissues described in [9]. In this manner, a quasi-omnidirectional and wideband antenna within the UWB frequency range was achieved. Hence, a reliable measurement campaign within UWB frequency range has been carried out. To assess the miniaturized antenna performance as well as the characterization of UWB in-body channel, we have compared the relative received power obtained with the miniaturized antenna with that obtained in [10] with a larger antenna [11] in two scenarios.

The remainder of the paper is organized as follows. In section II, the miniaturization procedure is detailed. Section III details the measurement methodology. In section IV, UWB channel propagation results emulating in-body scenarios using the miniaturized antenna will be compared with those obtained in a previous campaign. In section V, the conclusions of this work are summarized.

II. IN-BODY DESIGNING STAGE

A. Simulation Setup

The design procedure of in-body antennas should be different to that in free space. In literature, there can be found studies where the antenna is designed in free space in a first stage [7]. The in-body antenna is designed to work in high frequencies since, when it is implanted in a human tissue, the wavelength is shorter [8]:

$$\lambda_{eff} = \frac{\lambda_0}{\mathrm{Re}\left[\sqrt{\varepsilon_r}\right]} = \frac{\lambda_0}{\mathrm{Re}\left[\sqrt{\varepsilon_r^{'} - j\varepsilon_r^{''}}\right]}, \quad (1)$$

where λ_{eff} is the wavelength in body tissue, λ_0 is the wavelength in free space, ε_r is the complex relative permittivity, $\varepsilon_r^{'}$ is the dielectric constant and $\varepsilon_r^{''}$ is the loss factor. Thus, it could be considered a shortening factor in the design stage as proposed in [7]. However, this technique is not always efficient due to the fact that design considerations were taken in order to work in free space. Hence, the real radiation parameters of in-body antennas can vary dramatically.

In this work, the antenna was wrapped with a human muscle layer since the initial designing stage. For this purpose, an UWB planar monopole with CPW-feeding and circular patch was proposed as a candidate to apply this direct optimization approach. This kind of antenna presents a really compact structure, omnidirectional radiation pattern and broadband characteristics in free space [12].

Rogers 4003 dielectric substrate was chosen, which has a relative permittivity of 3.28 and a thickness of 0.813 mm. To keep the characteristics of this kind of antennas, several optimization techniques were considered. The bends in the ground plane were thoroughly studied in order to keep the omnidirectional radiation pattern into the human muscle tissue. Furthermore, a specific gap between the patch and the ground plane was carefully chosen in order to widen the bandwidth (L_b = 1 mm). Moreover, the shape of the patch was elliptical in contrast to [12] to enlarge the bandwidth as well. The rest of antenna dimensions are depicted in Fig. 1.

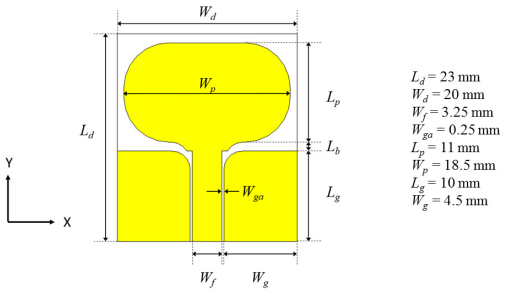

Fig. 1. UWB optimized planar antenna dimensions.

In Fig. 2 the simulation in CST of the gain pattern in the XZ-plane is shown. The simulations were performed by considering the theoretical values of the permittivity for the human muscle tissue reported in [9]. From Fig. 2, one can observe that the antenna exhibits a quasi-omnidirectional radiation pattern in XZ-plane at UWB frequencies. Hence, it can be checked that the antenna can keep omnidirectional radiation pattern within UWB frequencies by using the aforementioned miniaturization procedure.

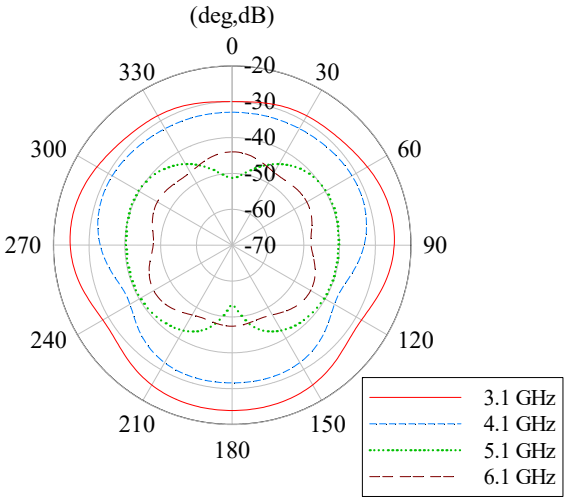

Fig. 2. Gain pattern of the miniaturized antenna in the human muscle tissue at 3.1, 4.1, 5.1 and 6.1 GHz.

B. Testing

The proposed CPW-Fed antenna, which is located in the center of Fig. 3, was fabricated and measured at our research facilities. Hereinafter, we refer to this antenna as the miniaturized antenna. At the left of the miniaturized antenna, a larger UWB patch antenna (50 x 40 mm^2) described in [11] and used in [10] as implanted antenna is depicted. Hereinafter, this antenna will be referred as the large antenna. The miniaturized antenna has been reduced by a factor of nearly 2.2 times with respect to the dimensions of the large antenna.

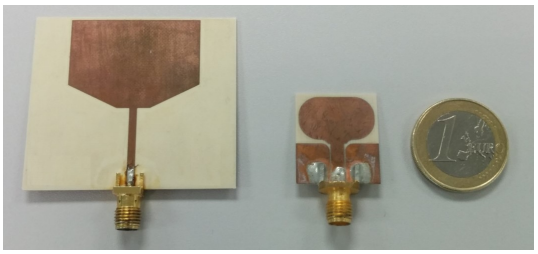

Fig. 3. Miniaturized UWB antenna.

After the manufacturing process, the antenna matching within the frequency range of interest should be checked. To achieve this goal, an alternative compound with electromagnetic behaviour close to that of the body tissues was used. In particular, a sucrose solution ($C_{12}H_{22}O_{11}$/1.0M), that emulates the human muscle electromagnetic behaviour within UWB frequency range 3.1-10.6 GHz, was prepared according to [13]. Hereinafter we refer to this solution as the phantom. This phantom is a fair imitation of the complex relative permittivity of the human muscle tissue. In order to measure the return loss (S_{11}), the antenna was submerged at a depth of 8 cm into the

phantom which was poured into an extruded polystyrene foam (Styrofoam™) container. The polystyrene container dimensions were 22 x 22 x 16 cm^3 with a wall thickness of 40 mm. The antenna was previously covered and isolated with a layer of Nitrile Butadiene Rubber (NBR) to avoid physical contact between the submerged antenna and the phantom. Subsequently, the antenna was connected to a Keysight Technologies™ ENA E5072A Vector Network Analyzer (VNA) whose maximum working frequency is 8.5 GHz. Besides, the VNA was calibrated through a full port calibration within the entire frequency band 3.1-8.5 GHz.

The simulated and measured results for the S_{11} are depicted in Fig. 4. It should be highlighted that the three curves exhibit a similar behaviour within all frequency points. Also, emphasize that all values are below -10 dB in the three cases. Therefore, it can be concluded that the miniaturization approach proposed in this work keeps the antenna matching within the entire frequency band.

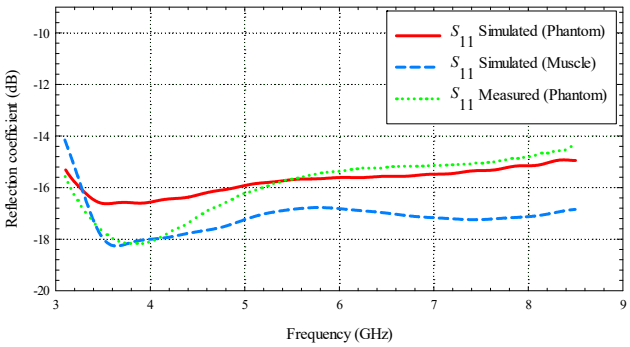

Fig. 4. Measured and simulated return loss within 3.1 – 8.5 GHz.

Besides, it should be pointed out that the miniaturized antenna exhibits very low radiation efficiency due to the high losses of the surrounding medium. These losses are in part responsible for the low S_{11} values and for the broad matching bandwidth of the antenna. However, as will be shown in section IV, despite the low efficiency of the miniaturized antenna, the received power values can be high enough to establish a communication channel in different scenarios.

III. Propagation Measurement Setup

A. Experimental setup

Regarding the location of the antennas, two different scenarios were considered:

- In-Body to On-Body (IB2OB), where the implanted antenna is placed into the body whereas the on-body antenna is located over the skin.
- In-Body to Off-Body (IB2OFF), where the implanted antenna is placed into the body whereas the off-body antenna is moved away from the body surface.

These two scenarios were emulated by using the setup depicted in Fig. 5.

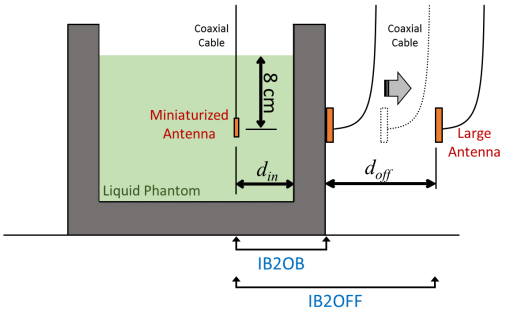

Fig. 5. Measurement Setups for each scenario.

In order to assess the performance of the miniaturized antenna, the measurement campaign reported in [10] was replicated by changing the in-body antenna for our miniaturized antenna. That is, the inner antenna used in the setup depicted in Fig. 5 was the miniaturized antenna, meanwhile in the same phantom setup described in [10] the large antenna was used as implanted antenna. In both cases, another large antenna with the same features was used as receiving antenna.

In order to avoid physical contact with the phantom, the implantable antenna was covered again with a layer of NBR and submerged into the phantom at a depth of 8 cm. In each scenario, the external antennas were placed in a vertical position as well as properly oriented to achieve a co-polarized mode. The transmitting and receiving antennas were connected to port 1 and port 2 of the VNA, respectively.

Regarding IB2OB scenario, the submerged antenna was moved away from the internal container face, whereas the on-body antenna was placed and fixed outside over the container wall. The spacing between the internal container face and the inner antenna was d_{in}. The thickness of the container wall can be disregarded as proposed in [14]. The measurements were made with an initial antenna separation of d_{in} = 20 mm, which was increased in steps of 10 mm up to 80 mm.

Considering the IB2OFF scenario, the submerged antenna was fixed to a distance of d_{in} = 40 mm into the phantom, whereas the off-body antenna was moved away of the external container face. The distance between the external container face and the off-body antenna was d_{off}.

B. Measurement methodology

In each measurement, the forward transmission coefficient, S_{21}, for each distance was obtained. The VNA output power was set to 8 dBm and the resolution bandwidth was set to f_{IF} = 3 kHz. Since the receiving antenna was located over the container wall in IB2OB and further away in IB2OFF, the noise floor varies slightly between scenarios. This can be explained by the fact that the antenna characteristics change as the distance between receiving antenna and the body surface is varied [15]. The measurement campaign was carried out within 3.1 to 8.5 GHz with N = 20001 resolution points in each snapshot resulting in a frequency resolution of Δf = 270 kHz. Besides,

five snapshots of the channel were stored for each separation distance in order to enhance the signal-to-noise ratio (SNR). Moreover, the VNA was calibrated through a thru-calibration within 3.1–8.5 GHz.

IV. Results

From measurements, we obtained the $\tilde{S}_{21}(f,d,k)$ where f is the frequency value, k is the snapshot number and d is the distance between antennas. Before the measurements processing, k = 5 snapshots were averaged to obtain $\tilde{S}_{21}(f,d)$. Thus, the relative received power as a function of frequency for a given separation distance between antennas was computed as:

$$P(f,d) = \left|\tilde{S}_{21}(f,d)\right|^2 \quad (2)$$

A. IB2OB

Fig. 6 depicts the received power obtained from each pair of antennas in the IB2OB scenario. From this figure, one can observe that the noise level was around -120 dBm.

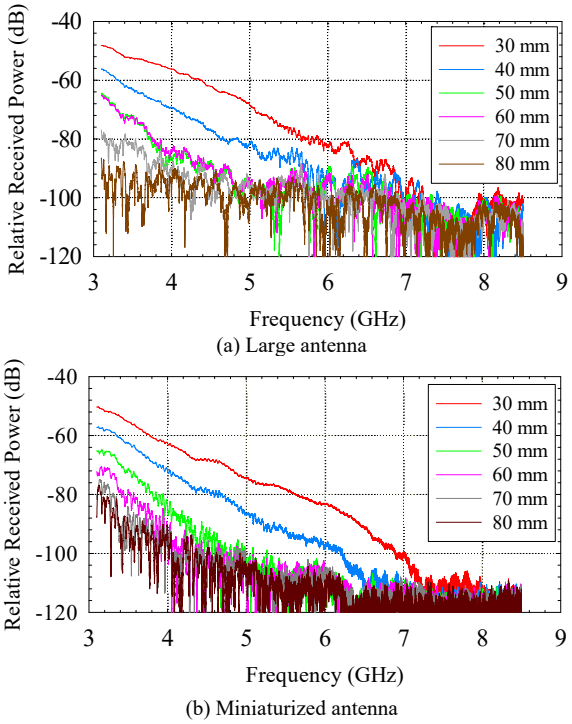

(a) Large antenna

(b) Miniaturized antenna

Fig. 6. Relative received power as a function of the frequency in the IB2OB scenario for different values of $d = d_i$.

From the results, one can observe that the frequency responses of the channel are very similar, especially when the distance between antennas is lower than 50 mm. In both cases, it can be noted that, approximately, the frequency response of the channel decreases linearly with frequency. On one hand, the frequency drop is explained by the fact that the antenna gain decreases with the increment of frequency (see Fig. 2). On the other hand, this drop is also related to the propagation medium, since the received power always decreases as the frequency increases. Furthermore, taking into account the losses of biological tissues [9] and liquid phantom [13], this frequency drop is higher. Besides, the slope is steeper as the separation distance between antennas increases. For instance, using the large antenna (Fig. 6(a)) for a separation distance of d_{in} = 40 mm, the received power decreases from -56.3 dB at 3.1 GHz to -70.7 dB at 4.1 GHz, whereas for a separation distance of d_{in} = 50 mm it decreases from -64.7 dB to -85.1 dB in the same frequency points. In the same manner, considering the miniaturized antenna (Fig. 6(b)), the power decreases from -57.1 dB to -73.6 dB for d_{in} = 40 mm and from -65.1 dB to -86.3 dB for d_{in} = 50 mm. Therefore, comparing the power decay with frequency of each pair of antennas within the frequency band 3.1-4.1 GHz, a difference of 2.1 dB for d_{in} = 40 mm and 4.7 dB for d_{in} = 50 mm is obtained, being the received power higher when the large antenna is used.

When the spacing between antennas is higher than 50 mm, the behaviour of the received power varies depending on the inner antenna used. The received power drops considerably as the separation distance between antennas is increased when using the large antenna. On the contrary, the received power obtained in case of the miniaturized antenna does not almost decrease as the distance between antennas increases. Moreover, the received power is around the noise floor for frequencies above 6.5 GHz using both transmitter antennas.

B. IB2OFF

Fig. 7 shows the relative received power as a function of frequency in the IBOFF scenario. It can be observed that the noise level was approximately at -110 dBm.

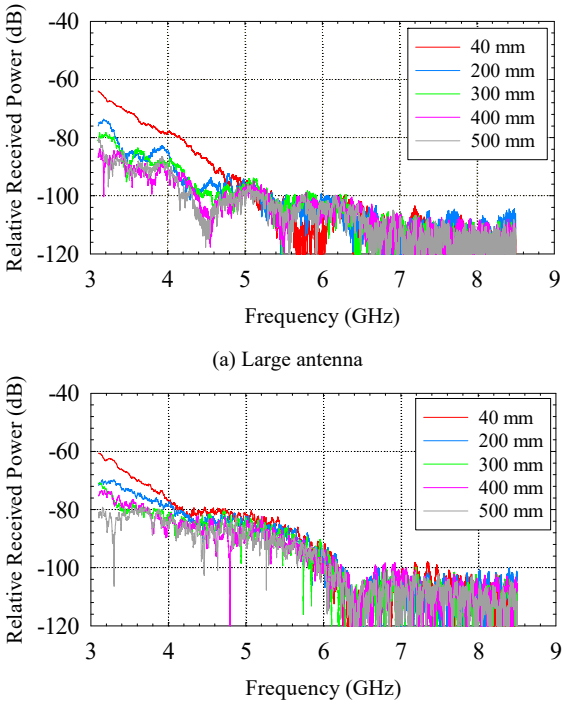

(a) Large antenna

(b) Miniaturized antenna

Fig. 7. Relative received power as a function of the frequency in the IB2OFF scenario for different values of $d = d_{off}$.

Comparing the received power depending on the inner antenna used, the power decays stepper in case of using the large antenna. Besides, the received power is higher using the miniaturized antenna from 3.1 to 6 GHz for all distances. One can also observe how the power response with frequency has a smoother decrease from 4 to 6 GHz in case of using the miniaturized antenna. For both antennas, the received power does not vary significantly when d_{off} is increased. This is explained by the fact that, in this scenario, the increments of d_{off} are performed being the air the propagation medium but being fixed the inner antenna. On the contrary, the relative received power for IB2OB scenario decreased considerably with the increments of d_{in} since, in that case, the outer antenna was fixed and the inner antenna was moved inside the phantom. Besides, it can be noted that using both antennas the relative received power is around the noise floor above 6.5 GHz.

V. Conclusions

In this paper, an UWB in-body channel measurements when using an antenna miniaturization procedure which keeps an omnidirectional radiation pattern as well as the operation bandwidth was presented. To achieve this goal, a well-known UWB CPW-Fed antenna was directly miniaturized and optimized taking into account the dielectric properties of human muscle tissue as the initial designing stage. Thus, the in-body antenna maintained its broadband characteristics as well as an omnidirectional radiation pattern. Next, in order to assess the miniaturization on the antenna, the UWB in-body channel was characterized. Thus, a set of phantom-based measurements of the UWB in-body channel within 3.1-8.5 GHz was performed in order to assess the effect of miniaturization on the channel performance. The obtained results from the miniaturized antenna in comparison with those obtained in the same conditions for a double-size UWB monopole antenna were analysed.

As the spacing between antennas increased, the received power in case of the miniaturized antenna as a function of frequency did not almost change. Regarding the IB2OFF scenario, the received power was higher when using the miniaturized antenna. Thus, our results evidenced that the both antennas had a similar behaviour in the case of in-body to on-body scenario for distances between antennas below 50 mm. The presented results evidenced the positive impact of designing the in-body antenna considering the propagation medium from the initial designing stage. Hence, an UWB antenna which maintains an omnidirectional radiation pattern and its bandwidth can be achieved. Future work should be focused on the validation of these results in a non-homogenous medium according to a realistic transmission through the human body tissues.

Acknowledgment

This work was supported by the Ministerio de Economía y Competitividad, Spain (ref. TEC2014-60258-C2-1-R, TEC2014-56469-REDT), by the European FEDER funds.

References

[1] W. G. Scanlon, J. B. Burns, and N. E. Evans, "Radiowave propagation from a tissue-implanted source at 418 MHz and 916.5 MHz," *IEEE Trans. Biomed. Eng.*, vol. 47, no. 4, pp. 527–34, Apr. 2000.

[2] R. Chavez-Santiago, K. Sayrafian-Pour, A. Khaleghi, K. Takizawa, J. Wang, I. Balasingham, *et al.*, "Propagation models for IEEE 802.15.6 standardization of implant communication in body area networks," *IEEE Commun. Mag.*, vol. 51, no. 8, pp. 80–87, Aug. 2013.

[3] P. A. Floor, R. Chavez-Santiago, S. Brovoll, Ø. Aardal, J. Bergsland, O.-J. H. N. Grymyr, *et al.*, "In-Body to On-Body Ultra Wideband Propagation Model Derived from Measurements in Living Animals," *IEEE J. Biomed. Heal. Informatics*, vol. 19, no. 3, pp. 1–1, 2015.

[4] A. Khaleghi, R. Chávez-Santiago, and I. Balasingham, "Ultra-wideband statistical propagation channel model for implant sensors in the human chest," *IET Microwaves, Antennas & Propag.*, vol. 5, no. 15, p. 1805, 2011.

[5] P. Soontornpipit, C. M. Furse, and Y. C. Chung, "Design of Implantable Microstrip Antenna for Communication With Medical Implants," *IEEE Trans. Microw. Theory Tech.*, vol. 52, no. 8, pp. 1944–1951, Aug. 2004.

[6] S. A. Kumar and T. Shanmuganantham, "Implantable CPW fed slot monopole antenna for biomedical applications," in *IEEE International Conference on Computational Intelligence and Computing Research*, 2012, pp. 1–4.

[7] Q. Wang, K. Wolf, and D. Plettemeier, "An UWB capsule endoscope antenna design for biomedical communications," in *3rd International Symposium on Applied Sciences in Biomedical and Communication Technologies (ISABEL 2010)*, 2010, pp. 1–6.

[8] P. S. Hall and Y. Hao, "Antennas and propagation for body-centric wireless communications," 2006, p. 258.

[9] C. Gabriel, "Compilation of the Dielectric Properties of Body Tissues at RF and Microwave Frequencies.," Brooks Air Force, N.AL/OE-TR- 1996-0037, San Antonio, TX, 1996.

[10] C. Garcia-Pardo, R. Chavez-Santiago, N. Cardona, and I. Balasingham, "Experimental UWB frequency analysis for implant communications," in *37th Annual International Conference of the IEEE Engineering in Medicine and Biology Society (EMBC)*, Milano, 2015, pp. 5457–5460.

[11] C. Tarin, P. Marti, L. Traver, N. Cardona, J. A. Diaz, and E. Antonino, "UWB Channel Measurements for Hand-Portable Devices: A Comparative Study," in *IEEE 18th International Symposium on Personal, Indoor and Mobile Radio Communications*, 2007, pp. 1–5.

[12] C. C. Chian, "CPW-fed circular disc monopole antenna for UWB applications," in *IEEE International Workshop on Antenna Technology (IWAT): Small Antennas and Novel Metamaterials, 2005.*, 2005, pp. 505–508.

[13] H. Yamamoto, J. Zhou, and T. Kobayashi, "Ultra Wideband Electromagnetic Phantoms for Antennas and Propagation Studies," *IEICE Transactions on Fundamentals of Electronics, Communications and Computer Sciences*, vol. E91-A, no. 11, pp. 3173–3182, Nov. 2008.

[14] R. Chavez-Santiago, C. Garcia-Pardo, A. Fornes-Leal, A. Valles-Lluch, G. Vermeeren, W. Joseph, *et al.*, "Experimental Path Loss Models for In-Body Communications within 2.36-2.5 GHz," *IEEE J. Biomed. Heal. informatics*, vol. 19, no. 3, pp. 930–937, Apr. 2015.

[15] T. Tuovinen, T. Kumpuniemi, K. Y. Yazdandoost, M. Hamalainen, and J. Iinatti, "Effect of the antenna-human body distance on the antenna matching in UWB WBAN applications," in *7th International Symposium on Medical Information and Communication Technology (ISMICT)*, 2013, pp. 193–197.